NEUROSCIENCE

Psychedelics promote neuroplasticity through the activation of intracellular 5-HT2A receptors

Maxemiliano V. Vargas[1,2], Lee E. Dunlap[2,3]†, Chunyang Dong[4]†, Samuel J. Carter[2,3],
Robert J. Tombari[2,3], Shekib A. Jami[5], Lindsay P. Cameron[1], Seona D. Patel[3], Joseph J. Hennessey[6],
Hannah N. Saeger[2,7], John D. McCorvy[6], John A. Gray[2,5,8], Lin Tian[2,5,9], David E. Olson[2,3,5,9]*

Decreased dendritic spine density in the cortex is a hallmark of several neuropsychiatric diseases, and the ability to promote cortical neuron growth has been hypothesized to underlie the rapid and sustained therapeutic effects of psychedelics. Activation of 5-hydroxytryptamine (serotonin) 2A receptors (5-HT2ARs) is essential for psychedelic-induced cortical plasticity, but it is currently unclear why some 5-HT2AR agonists promote neuroplasticity, whereas others do not. We used molecular and genetic tools to demonstrate that intracellular 5-HT2ARs mediate the plasticity-promoting properties of psychedelics; these results explain why serotonin does not engage similar plasticity mechanisms. This work emphasizes the role of location bias in 5-HT2AR signaling, identifies intracellular 5-HT2ARs as a therapeutic target, and raises the intriguing possibility that serotonin might not be the endogenous ligand for intracellular 5-HT2ARs in the cortex.

Dysregulation of the cortex has been hypothesized to play an important role in the pathophysiology of mental illnesses such as depression and often manifests as structural changes, including decreased dendritic arbor complexity and reduced dendritic spine density (1–3). Traditional antidepressants, such as selective serotonin reuptake inhibitors (SSRIs), can rescue these deficits after chronic treatment, although it seems that their effects may be independent of serotonin and perhaps involve the activation of tropomyosin receptor kinase B (TrkB) signaling (4, 5). A class of therapeutic compounds known as psychoplastogens (6) are differentiated from SSRIs by their ability to produce both rapid and sustained effects on structural plasticity and behavior after a single administration (7). Psychoplastogens include both ketamine and serotonergic psychedelics, although their primary targets are distinct (7).

Psychedelics are 5-hydroxytryptamine (serotonin) 2A receptor (5-HT2AR) agonists that can lead to profound changes in perception, cognition, and mood (8). Recent evidence suggests that they promote cortical structural and functional neuroplasticity through activation of 5-HT2ARs (9, 10). The mechanism by which 5-HT2AR activation leads to changes in neuronal growth is still poorly defined, although it appears to involve TrkB, mechanistic target of rapamycin (mTOR), and AMPA receptor signaling (11). It is currently unclear why some 5-HT2AR ligands can promote neuroplasticity and produce sustained therapeutic behavioral responses in the absence of hallucinogenic effects, whereas other 5-HT2AR agonists do not promote plasticity at all (12–15). Indeed, serotonin itself does not produce psychedelic-like effects on neuronal growth when administered to cortical cultures (9). This enigmatic finding cannot be easily explained by traditional biased agonism because serotonin is a balanced agonist of the 5-HT2AR that exhibits high potency and efficacy for activating both heteromeric guanine nucleotide–binding protein (G protein) and β-arrestin pathways (16, 17).

Unlike psychedelics, the physicochemical properties of serotonin prevent it from entering cells by passively diffusing across nonpolar membranes (8). Thus, we reasoned that another form of functional selectivity, known as location bias, might explain the difference in cellular signaling elicited by serotonin and psychedelics (18, 19). Here, we leveraged both chemical design and genetic manipulation to test the hypothesis that activation of an intracellular population of 5-HT2ARs is necessary for 5-HT2AR ligands to induce cortical structural plasticity and produce antidepressant-like behavioral responses.

Lipophilicity correlates with psychoplastogenicity

To firmly establish the role of 5-HT2AR activation in psychedelic-induced spinogenesis, we administered 5-methoxy-N,N-dimethyltryptamine (5-MeO) to wild-type (WT) and 5-HT2AR knockout (KO) mice (20) and assessed structural and functional changes in layer 5 pyramidal neurons of the prefrontal cortex (PFC) 24 hours [...] (fig. S1, A to C). Golgi-Cox staining revealed that 5-MeO increased spine density in both male and female animals, and this effect was absent in 5-HT2AR KO mice (fig. S1, A and B). Furthermore, ex vivo electrophysiology confirmed that 5-HT2AR activation is necessary for 5-MeO to produce sustained increases in both the frequency and amplitude of spontaneous excitatory postsynaptic currents (sEPSCs) (fig. S1C).

Next, we determined how the structures of 5-HT2AR ligands affect their abilities to promote neuronal growth by treating embryonic rat cortical neurons with serotonin, tryptamine (TRY), 5-methoxytryptamine (5-MeO–TRY), and their corresponding N-methyl and N,N-dimethyl congeners (Fig. 1A) before assessing neuronal morphology by means of Sholl analysis (21). Ketamine was used as a positive control because of its known ability to induce structural plasticity in this assay (9). These structure-activity relationship (SAR) studies revealed that increasing N-methylation led to an enhanced ability to promote neuronal growth, with the N,N-dimethyl compounds increasing dendritic arbor complexity to the greatest extent (Fig. 1, B to D).

Increasing N-methylation is known to affect the efficacy of 5-HT2AR signaling, so we attempted to correlate psychoplastogenic efficacy across a range of 5-HT2AR ligands with efficacy in a traditional [³H]–inositol phosphates (IP) accumulation assay (Fig. 1E) (22). Notably, we did not observe a positive correlation between psychoplastogenic effects and ligand efficacy. Indeed, there seemed to be a non-significant inverse correlation between [³H]-IP accumulation and dendritogenesis efficacy (Fig. 1E). To avoid potential issues associated with the amplification of secondary messengers, we used psychLight2, a fluorescent biosensor that is capable of directly detecting changes in 5-HT2AR conformation (14). PsychLight2 efficacy closely mirrored that observed by using [³H]-IP accumulation assays, although psychLight2 efficacy exhibited an even stronger anticorrelation with dendritogenesis efficacy (P = 0.06) (Fig. 1F). Lastly, we used bioluminescence resonance energy transfer (BRET) assays to directly measure G_q activation or β-arrestin-2 recruitment (fig. S2) (23). Both measures of 5-HT2AR efficacy exhibited a strong negative correlation with psychoplastogenicity (Fig. 1, G and H). Moreover, both G_q activation and β-arrestin recruitment correlated well with psychLight efficacy [coefficient of determination (R^2) = 0.9; P < 0.0001 and P = 0.0006, respectively] (Fig. 1I). Negative correlation between 5-HT2AR efficacy and psychoplastogenicity should be interpreted with caution because this relationship may only apply to tryptamine-based ligands or compounds that exhibit a threshold level of 5-HT2AR activation.

[1]Neuroscience Graduate Program, University of California, Davis, Davis, CA 95618, USA. [2]Institute for Psychedelics and Neurotherapeutics, University of California, Davis, Davis, CA 95618, USA. [3]Department of Chemistry, University of California, Davis, Davis, CA 95616, USA. [4]Biochemistry, Molecular, Cellular, and Developmental Biology Graduate Program, University of California, Davis, Davis, CA 95616, USA. [5]Center for Neuroscience, University of California, Davis, Davis, CA 95618, USA. [6]Department of Cell Biology, Neurobiology, and Anatomy, Medical College of Wisconsin, Milwaukee, WI 53226, USA. [7]Pharmacology and Toxicology Graduate Program, University of California, Davis, Davis, CA 95616, USA. [8]Department of Neurology, School of Medicine, University of California, Davis, Sacramento, CA 95817, USA. [9]Department of Biochemistry and Molecular Medicine, School of Medicine, University of California, Davis, Sacramento, CA 95817, USA.
*Corresponding author. Email: deolson@ucdavis.edu
†These authors contributed equally to this work.

Nitrogen methylation of 5-HT2AR ligands structurally related to serotonin is known to result in partial agonism (*22*), but it also has a profound effect on their physicochemical properties. These compounds display a wide range of lipophilicities that ranged from highly polar molecules such as serotonin to relatively nonpolar compounds such as *N,N*-dimethyltryptamine (DMT). Using calculated LogP (cLogP) values, we observed a significant positive correlation with psychoplastogenic effects—more lipophilic agonists exhibited greater abilities to promote structural plasticity than polar compounds (Fig. 1J). This relationship was evident within the TRY, serotonin, and 5-MeO–TRY scaffolds. The finding that lipophilicity was a better predictor of psychoplastogenicity than 5-HT2AR activation led us to hypothesize that an intracellular pool of 5-HT2ARs in cortical neurons might be responsible for psychedelic-induced neuronal growth.

Primary localization of 5-HT2ARs in cortical neurons is intracellular

Although most G protein–coupled receptors (GPCRs) are believed to be localized primarily to the plasma membrane, several exhibit substantial intracellular localization (*24–27*). In vitro and ex vivo experiments have also established the existence of large intracellular pools of 5-HT2ARs in various cell types in the absence of a ligand (*28–31*). To compare 5-HT2AR localization patterns between cell types, we expressed a Myc–5-HT2AR–enhanced cyan fluorescent protein (ECFP) construct in both human embryonic kidney 293T (HEK293T) cells and cortical neurons, performed live-cell imaging, and assessed colocalization with a membrane dye (Cellbrite Steady) that labels the extracellular side of the plasma membrane. Because overexpression of tagged receptor constructs might alter trafficking and localization, we included several controls. We used a β2 adrenergic receptor tagged with ECFP (β2AR-ECFP) as a GPCR that is canonically described as being plasma membrane bound, and we used an ECFP construct to establish the localization of a fluorescent protein that is not tagged to a GPCR (*32, 33*).

When expressed in HEK293T cells that were cultured in the absence of serum, 5-HT2ARs and β2ARs exhibited similar cellular expression patterns (Fig. 2A) and possessed correlation coefficients with the plasma membrane marker that were not statistically different (Fig. 2B). However, these two GPCRs displayed distinct localization patterns in neurons. In cortical neurons, β2AR expression was more highly correlated with the plasma membrane marker than was 5-HT2AR expression (Fig. 2B), which demonstrates that overexpression of a GPCR in cortical neurons does not necessarily lead to intracellular localization. The extent of overexpression was similar for 5-HT2ARs and β2ARs in both HEK293T cells and cortical neurons (fig. S3A). We performed these localization experiments without serum in the culturing media because serum contains serotonin, which can lead to agonist-induced changes in trafficking and localization (fig. S3, B and C). In both neurons and HEK293T cells,
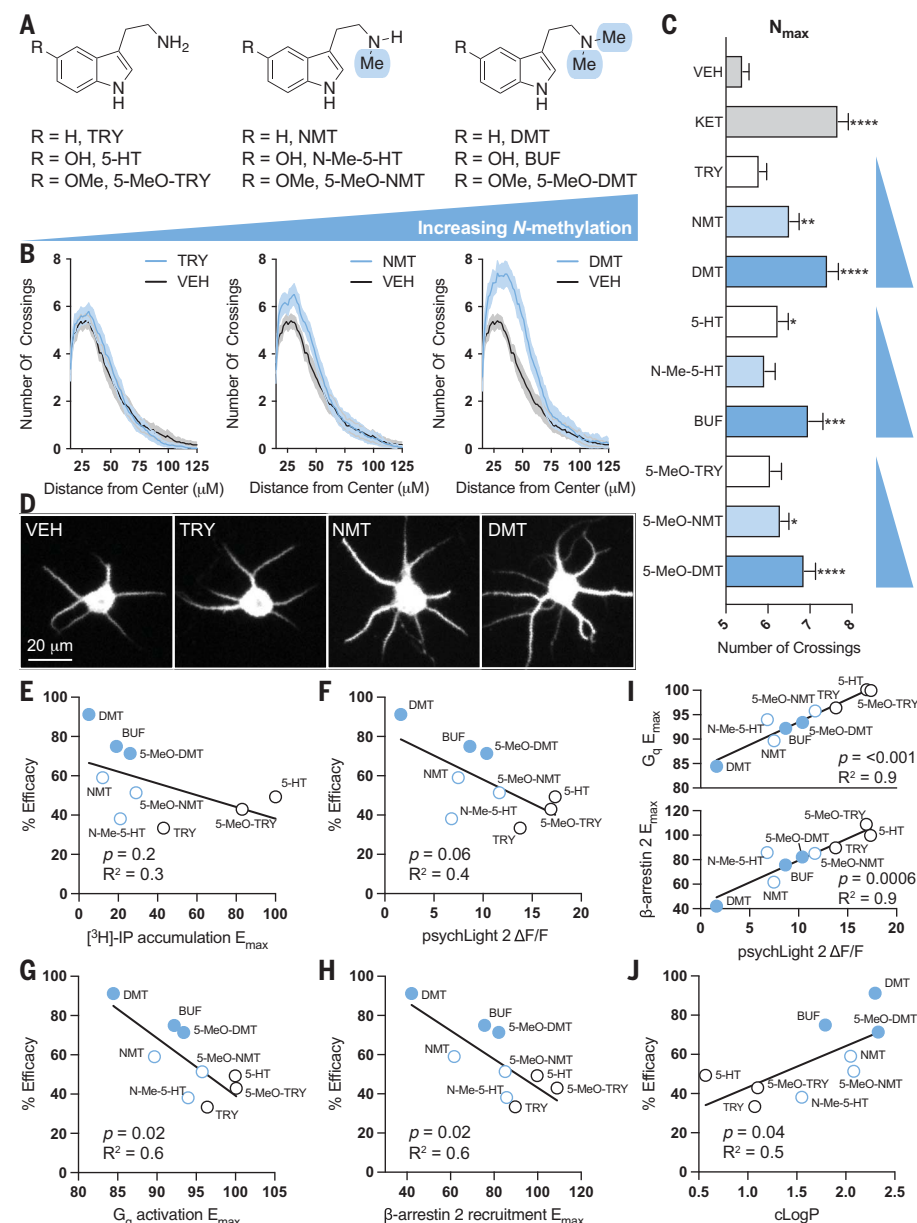

Fig. 1. Compound-induced neuronal growth correlates with ligand lipophilicity. (**A**) Chemical structures of serotonin, TRY, and 5-MeO–TRY as well as their corresponding *N*-methyl and *N,N*-dimethyl analogs. 5-HT, serotonin; BUF, bufotenin; Me, methyl; N-Me-5-HT, *N*-methylserotonin; NMT, *N*-methyltryptamine. (**B**) Sholl analysis demonstrates that increasing N-methylation leads to a concomitant increase in dendritic arbor complexity. The shaded area represents 95% confidence intervals. Sholl plots were generated from rat embryonic cortical neurons (DIV6) treated with compounds (10 μM). VEH, vehicle. (**C**) Maximum numbers of crossings (N_{max}) of the Sholl plots in (B) (N = 45 to 64 neurons per treatment). Error bars represent standard error of the mean. KET, ketamine. (**D**) Widefield images of rat embryonic cortical neurons (DIV6) treated with compounds (10 μM). (**E** to **J**) Correlation plots of Sholl analysis percent efficacy (N_{max} values relative to 10 μM ketamine as the positive control) versus [³H]-IP accumulation (E), activation of psychLight2 (F), G_q activation (G), β-arrestin recruitment (H), or calculated LogP (J). PsychLight2 activation correlates well with both G_q activation and β-arrestin recruitment (I). Compounds were treated at 10 μM. Data for [³H]-IP accumulation were obtained from literature values (*22*). *$p < 0.05$, **$p < 0.01$, ***$p < 0.001$, and ****$p < 0.0001$, as compared with VEH controls [one-way analysis of variance (ANOVA) followed by Dunnett's multiple comparisons test]. R^2 values were calculated through simple liner regression. ΔF/F, change in fluorescence intensity relative to the baseline fluorescence intensity; E_{max}, maximum effect.
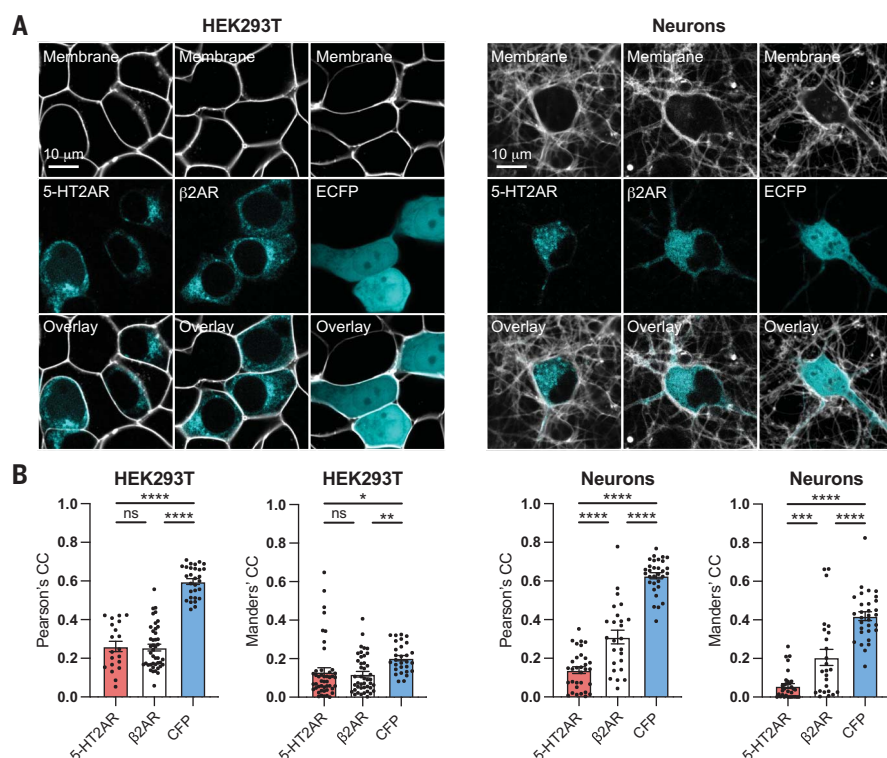
Fig. 2. Cortical neurons express intracellular 5-HT2A receptors. (**A**) Live-cell images of HEK293T cells and rat embryonic cortical neurons (DIV6) expressing Myc–5-HT2AR–CFP, β2AR-ECFP, or ECFP. Signals from the fluorescent protein and fluorescent plasma membrane marker (Cellbrite Steady) are shown in cyan and white, respectively. The expression patterns of 5-HT2ARs and β2ARs are comparable in HEK293T cells. However, in neurons, β2ARs exhibit higher expression on the plasma membrane than 5-HT2ARs. The expression of ECFP is diffuse in both HEK293T cells and cortical neurons. (**B**) Pearson's correlation coefficients (Pearson's CCs) and Manders' colocalization coefficients (Manders' CCs) quantify the extent of colocalization between MYC–5-HT2AR–CFP, β2AR-ECFP, or ECFP and the fluorescent plasma membrane marker (N = 20 to 43 cells per group). Error bars represent standard error of the mean. ns is not significant, $*p < 0.05$, $**p < 0.01$, $***p < 0.001$, and $****p < 0.0001$; bars indicate comparisons between data (one-way ANOVA followed by Tukey's multiple comparisons test).

the expression patterns of the tagged GPCRs were markedly distinct from ECFP, which confirms that the GPCR component of the constructs dictates cellular localization. Expression of a FLAG–5-HT2AR construct in rat cortical neurons produced a similar intracellular localization pattern, which suggests that these tags do not substantially alter the localization patterns of the 5-HT2AR (*34*).

Bright punctate staining within neurons suggested that 5-HT2ARs were localized within intracellular compartments (Fig. 2A), so we performed additional immunocytochemistry experiments to assess the overlap with markers of various subcellular organelles (fig. S4). We observed a high level of 5-HT2AR colocalization with Rab5 and Rab7 in both HEK293T cells and neurons. Ras-related guanosine triphosphatases (GTPases) of the Rab family are known to regulate intracellular transport of GPCRs (*35*). We observed a very large difference in 5-HT2AR colocalization with the Golgi apparatus between neurons and HEK293T

cells, with the former exhibiting substantially higher correlation coefficients (fig. S4). The Golgi apparatus is a key regulator of GPCR signaling, and ligands can either passively diffuse into Golgi-localized receptor pools or gain access by facilitated transmembrane transport (*18, 36, 37*). Signaling from within the Golgi can be distinct, as is the case for opioid receptors (*38*).

To ensure that high 5-HT2AR colocalization with the Golgi was not an artifact of overexpression, we assessed native 5-HT2AR expression in neurons using one of the few validated 5-HT2AR antibodies (*30*). To confirm the antibody's specificity, we performed in-house validation by overexpressing 5-HT2ARs in HEK293T cells (fig. S5A) and we used mouse 5-HT2AR KO cortical neurons (fig. S5B). Next, we imaged rat embryonic cortical neurons that expressed only native 5-HT2ARs or overexpressed a Myc–5-HT2AR–ECFP construct. Longitudinal and transverse line scans indicated that Myc–5-HT2AR–ECFP expression closely mirrored the

native localization pattern of 5-HT2ARs (fig. S5, C and D).

Membrane permeability is required for psychedelic-induced neuroplasticity

Given that cortical neurons have a large pool of intracellular 5-HT2ARs, we next used chemical tools to determine whether activation of this intracellular population was essential for psychedelics to promote structural neuroplasticity. Chemical modification of the membrane-permeable ligands DMT, psilocin (PSI), and ketanserin (KTSN) converted them into highly charged membrane-impermeable congeners *N,N,N*-trimethyltryptamine (TMT), psilocybin (PSY), and methylated ketanserin (MKTSN), respectively (Fig. 3A). All of the charged species exhibited negative cLogP scores (fig. S6A) but retained affinity for 5-HT2ARs, as determined by radioligand competition binding experiments (fig. S6B). In psychLight2 assays, the membrane-impermeable analogs displayed comparable efficacies to their uncharged parent molecules with reduced potencies (fig. S6, C and D).

Next, we treated freshly dissected rat embryonic cortical neurons with DMT (1 μM) and PSI (1 μM) as well as their membrane-impermeable congeners in the presence and absence of electroporation. Electroporation creates temporary openings in the plasma membrane, which enables highly charged molecules to pass through and access the intracellular space. Although the membrane-permeable 5-HT2AR agonists were able to promote dendritogenesis regardless of whether electroporation was applied, the membrane-impermeable compounds could only promote neuronal growth when applied with electroporation (Fig. 3, B and C). Similarly, the membrane-permeable 5-HT2AR antagonist KTSN (treated in 10-fold excess at 10 μM) blocked DMT-induced plasticity both with and without electroporation; however, the membrane-impermeable antagonist MKTSN (10 μM) could only block DMT-induced neuronal growth when it was applied with electroporation (Fig. 3, B and C). By using more mature neurons (DIV15), we demonstrated that the membrane-permeable 5-HT2AR agonists increased dendritic spine density—another measure of structural neural plasticity—whereas the membrane-impermeable agonists did not (Fig. 3, D and E). KTSN was able to inhibit the effects of DMT and PSI on dendritic spine density, whereas MKTSN was not (fig. S7).

To further establish that membrane-permeable and -impermeable ligands target different populations of 5-HT2ARs, we performed an experiment in HEK293T cells that express psychLight1. The psychLight1 construct was chosen over psychLight2 because the former lacks an endoplasmic reticulum (ER) export sequence, which results in greater intracellular localization (*14*). PsychLight1-expressing HEK293T cells were pretreated with either
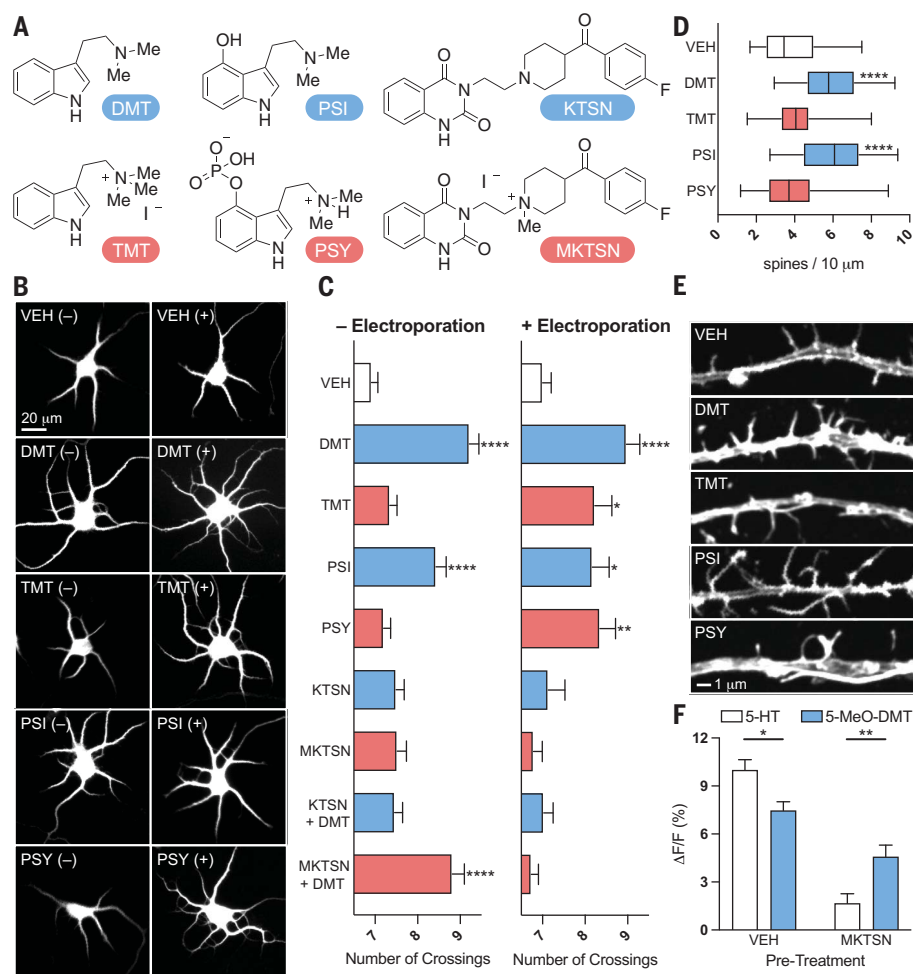
Fig. 3. Intracellular 5-HT2ARs mediate structural plasticity induced by serotonergic psychoplastogens.
(**A**) Structures of membrane-permeable (blue) and impermeable (red) compounds. (**B**) Widefield images of rat embryonic cortical neurons (DIV6) that were administered compounds with (+) and without (−) electroporation. (**C**) N_{max} values obtained from Sholl plots. Membrane-impermeable analogs of psychedelics (1 μM) only promote growth when administered with electroporation (N = 35 to 110 neurons per treatment). Unlike KTSN (10 μM), MKTSN (10 μM) only blocks psychedelic-induced plasticity when administered with electroporation (N = 45 to 109 neurons per treatment). (**D**) Membrane-impermeable agonists of 5-HT2ARs (1 μM) cannot promote spinogenesis in cultured embryonic rat cortical neurons (DIV15) (N = 30 to 34 neurons per treatment). (**E**) Confocal images of treated cortical neurons (DIV15). (**F**) HEK293T cells that expressed psychLight1 were pretreated with VEH or MKTSN (10 μM) before the administration of serotonin (10 μM) or 5-MeO–DMT (10 μM) (N = 41 to 54 cells per treatment). Error bars in (C) and (F) represent standard error of the mean. *$p < 0.05$, **$p < 0.01$, and ****$p < 0.0001$, as compared with VEH controls in (D) and (C) (one-way ANOVA followed by Dunnett's multiple comparisons test) or between indicated pairs of data in (F) (two-way ANOVA followed by Šídák's multiple comparisons test). For box-and-whisker plots in (D), the center line represents the median, box limits are upper and lower quartiles, and whiskers are minimum and maximum values.

vehicle or MKTSN to selectively antagonize the population of 5-HT2ARs that were expressed on the plasma membrane. Next, changes in psychLight1 fluorescence were measured after administration of the membrane-impermeable ligand serotonin or its membrane-permeable congener 5-MeO–DMT. Because serotonin is a full agonist, it induced a stronger response in the absence of antagonist compared with the partial agonist 5-MeO–DMT. Pretreatment with MKTSN resulted in a much larger reduction in the serotonin-induced psychLight1 signal compared with that induced by 5-MeO–DMT (Fig. 3F). Pretreatment with MKTSN could nearly fully antagonize the effect of serotonin. In sharp contrast, MKTSN only partially blocked the ability of 5-MeO–DMT to turn on psychLight1 fluorescence.

Because serotonin and 5-MeO–DMT exhibit different lipophilicities (cLogP values of 0.57

and 2.33, respectively), we reasoned that their abilities to displace [³H]–D-lysergic acid diethylamide (LSD) bound to the 5-HT2AR would depend on whether those receptors were exposed to the extracellular environment. Thus, we performed radioligand competition binding experiments using intact HEK293T cells that expressed Myc–5-HT2AR or psychLight2 as well as membrane preparations obtained from these systems. The inhibition constant (K_i) values for serotonin and 5-MeO–DMT were nearly identical when using membrane preparations or intact PSYLI2 cells, with HEK293T cells that stably expressed a 5-HT2AR construct with an ER export sequence resulting in a large proportion of the 5-HT2ARs being exposed to the extracellular environment (fig. S8). However, 5-MeO–DMT was an order of magnitude more potent than serotonin when using intact HEK293T cells that expressed large populations of both plasma membrane–bound and intracellular 5-HT2ARs (fig. S8).

To confirm that serotonin and 5-MeO–DMT can target distinct populations of 5-HT2ARs, we performed inositol monophosphate (IP1) assays in cortical neurons and HEK293T cells that expressed the Myc–5-HT2AR–ECFP construct. When the assay was performed in HEK293T cells that expressed Myc–5-HT2AR–ECFP, which display a large proportion of plasma membrane–bound 5-HT2ARs, serotonin and 5-MeO–DMT had comparable potencies and efficacies (fig. S9A). When the same experiment was performed in rat cortical neurons, serotonin failed to elicit an agonist response, although 5-MeO–DMT remained a potent agonist (fig. S9B).

Cellular import of serotonin leads to structural plasticity and antidepressant-like effects

If activation of intracellular 5-HT2ARs in cortical neurons is sufficient to promote structural plasticity, we hypothesized that serotonin should be able to promote cortical neuron growth if given access to the intracellular space. To test this hypothesis, we first treated cortical neurons with serotonin (1 μM) in the presence and absence of electroporation. Unlike ketamine (1 μM), serotonin was only able to promote cortical neuron growth when applied with electroporation (Fig. 4A). Next, we took advantage of the serotonin transporter (SERT), which can import serotonin from the extracellular environment (39). Endogenous expression of SERT is typically restricted to presynaptic terminals of neurons that emanate from the raphe, and thus, rat cortical neurons do not express appreciable levels of the transporter (40, 41). Embryonic rat cortical neurons were electroporated with an enhanced yellow fluorescent protein (EYFP)–tagged SERT construct under the control of the calcium/calmodulin-dependent protein kinase II (CaMKII) promoter to restrict expression to excitatory pyramidal neurons. Sparse transfection resulted in cultures
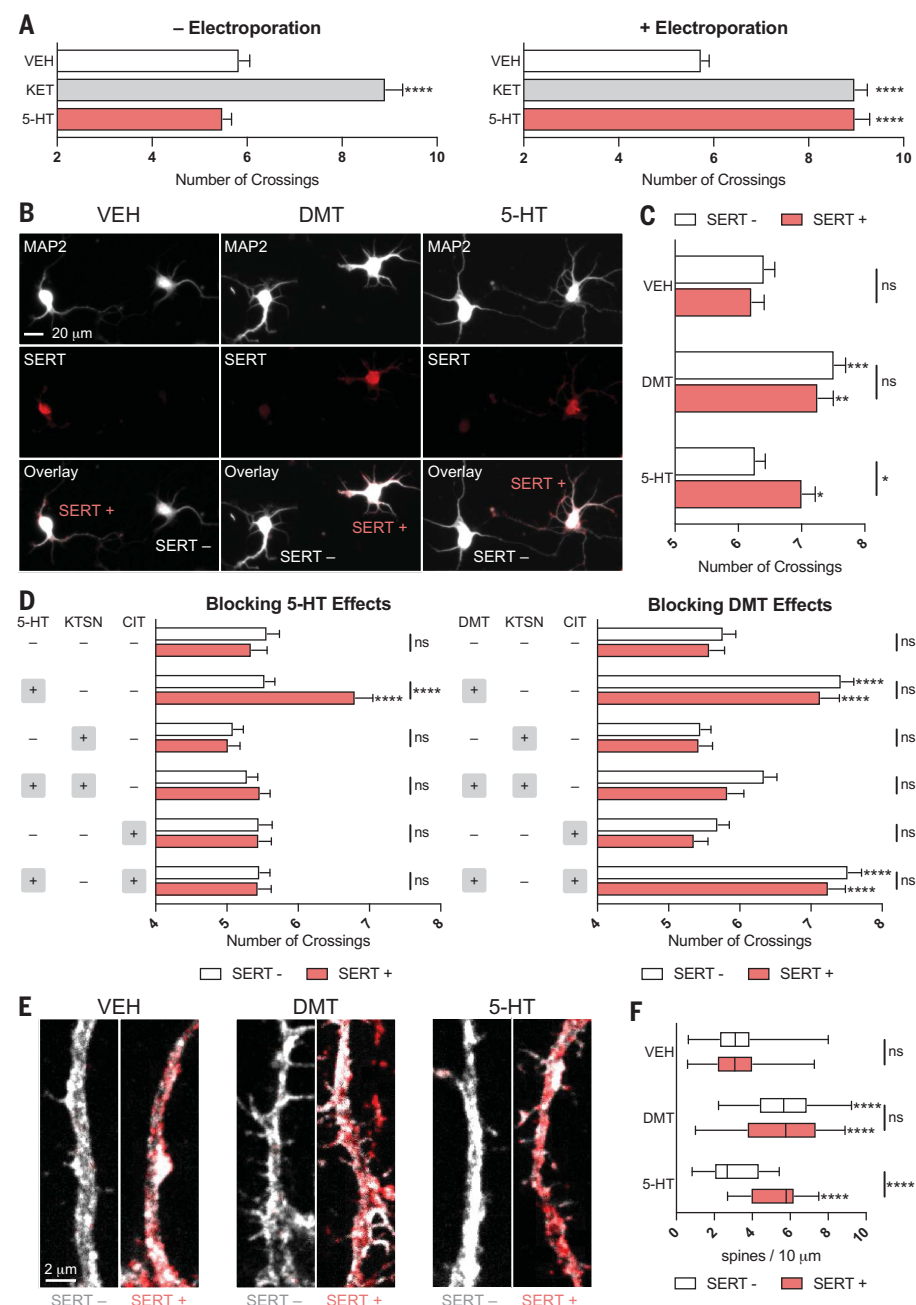
Fig. 4. Cellular uptake of serotonin induces structural plasticity in vitro. (**A**) Rat embryonic cortical neurons were administered compounds (1 μM) with (+) and without (−) electroporation. N_{max} values obtained from Sholl plots (DIV6) demonstrates that unlike ketamine, serotonin only promotes growth when administered with electroporation (N = 49 to 59 neurons per treatment). (**B**) Widefield images of embryonic rat cortical cultures (DIV6) sparsely transfected with CaMKII-SERT-EYFP and treated with compounds. (**C**) N_{max} values obtained from Sholl plots demonstrate that serotonin (10 μM) can only increase the dendritic arbor complexity of SERT-positive neurons, whereas DMT (10 μM) can promote the growth of both SERT-positive and SERT-negative neurons (N = 69 to 93 neurons per treatment). (**D**) KTSN pretreatment (10 μM) blocks the plasticity-promoting effects of serotonin (1 μM) in SERT-positive neurons and DMT (1 μM) in both SERT-positive and SERT-negative neurons. CIT (10 μM) only blocks the plasticity-promoting effects of serotonin (1 μM) in SERT-positive neurons (N = 59 to 100 neurons per treatment). (**E**) Confocal images of CaMKII-SERT-EYFP positive and negative dendrites (DIV15) treated with compounds (10 μM). (**F**) Serotonin only promotes spine growth in SERT-positive neurons (N = 11 to 35 neurons per treatment). Error bars in (A), (C), and (D) represent standard error of the mean. ns is not significant, *$p < 0.05$, **$p < 0.01$, ***$p < 0.001$, and ****$p < 0.0001$, as compared with VEH controls in (A) (one-way ANOVA followed by Dunnett's multiple comparisons test) or compared with VEH controls from the same genotype in (C), (D), and (F) (two-way ANOVA followed by Tukey's multiple comparisons test). For box-and-whisker plots in (F), the center line represents the median, box limits are upper and lower quartiles, and whiskers are minimum and maximum values.

that expressed both SERT-positive and SERT-negative neurons (Fig. 4B), which enabled us to compare the effects of serotonin on neurons capable of importing the monoamine with those that could not within the same cultures.

Treatment with the membrane-permeable psychedelic DMT (10 μM) resulted in greater dendritic arbor complexity and increased spine density in both SERT-positive and SERT-negative neurons (Fig. 4, B to F). Only SERT-positive neurons treated with serotonin (10 μM) displayed increased dendritogenesis and spinogenesis (Fig. 4, B to F). To ensure that serotonin-induced changes in structural neural plasticity were due to the engagement of intracellular 5-HT2Rs through serotonin importation from SERT, we performed similar experiments in the presence of the selective SERT inhibitor citalopram (CIT) and KTSN. When these experiments were performed in the presence of CIT (10 μM), the plasticity-promoting effects of serotonin (1 μM) on SERT-positive neurons were blocked (Fig. 4D). By contrast, CIT had no effect on the ability of DMT (1 μM) to promote the growth of SERT-positive or SERT-negative cortical neurons (Fig. 4D). In the presence of KTSN (10 μM), neither serotonin nor DMT could promote neuronal growth, which confirms that DMT and intracellular serotonin promote plasticity by means of 5-HT2AR receptors in vitro (Fig. 4D).

To determine whether intracellular serotonin could promote the growth of cortical neurons in vivo, we injected the medial PFC (mPFC) of Thy1–enhanced green fluorescent protein (EGFP) mice with either CaMKII-SERT-mCherry or CaMKII-mCherry. The mPFC was chosen as the injection site because it exhibits high levels of 5-HT2AR expression (28) and has been implicated in the antidepressant-like effects of psychoplastogens (42). After 3 weeks to enable construct expression (Fig. 5, A and B), both groups were administered (±)-para-chloroamphetamine [PCA, 5 mg/kg intraperitoneally (ip)], a selective serotonin-releasing agent (43). Dendritic spine density on mPFC pyramidal neurons was assessed 24 hours later. Animals that expressed SERT in the mPFC displayed significantly higher densities of dendritic spines after PCA administration as compared with mCherry controls (Fig. 5, C and D). Notably, PCA is not a 5-HT2AR agonist (fig. S10A), does not directly promote the growth of SERT-positive or SERT-negative cortical neurons in culture (fig. S10B), and does not induce a head-twitch response (HTR) in WT mice (fig. S10C).

Evidence suggests that psychoplastogen-induced structural plasticity in the mPFC might be related to sustained antidepressant-like effects in rodents (44). To probe for an antidepressant-like response that might be linked to neuroplasticity, we injected an adeno-associated virus (AAV) that contained a CaMKII-SERT-EYFP or CaMKII–green fluorescent protein (GFP)

construct into the mPFC of WT C57BL/6J mice (Fig. 5E and fig. S10D). After 3 weeks to allow for construct expression, both groups of mice underwent a novelty induced locomotion (NIL) test, and no differences in locomotion were observed (Fig. 5F). After 24 hours, mice were subjected to a forced swim test (FST) (7, 45). Again, we observed no differences between the mice that expressed SERT and those that expressed the GFP control (Fig. 5G). Two days later, we administered PCA (5 mg/kg ip), waited 24 hours, and then performed a second FST (Fig. 5G). The SERT-expressing mice exhibited a statistically significant HTR immediately after the administration of PCA as compared with the GFP control mice (fig. S10E), and they also displayed a significant reduction in immobility in the FST 24 hours after administration (Fig. 5G).

Discussion

Although GPCRs are traditionally viewed as initiators of signal transduction that originates at the plasma membrane, increasing evidence suggests that GPCR signaling from intracellular compartments can play important roles in cellular responses to drugs. Recently, location bias has been proposed to explain signaling differences between endogenous membrane-impermeable peptide ligands and membrane-permeable ligands of opioid receptors (38). Moreover, distinct ligand-induced signaling has been observed for plasma membrane–localized and intracellular populations of δ-opioid receptors (46). Here, we extend the concept of location bias to ligands of the 5-HT2AR.

A substantial proportion of 5-HT2ARs in cortical neurons are localized to the Golgi, and intracellular compartments such as the Golgi are slightly acidic compared with the cytosol and extracellular space. Thus, it is possible that protonation of psychedelics within the Golgi leads to retention and sustained signaling, which results in neuronal growth, even after transient stimulation (47). Persistent growth after the drugs have been removed from the extracellular space is a hallmark of serotonergic psychoplastogens (47, 48). Although the mechanistic details that link intracellular 5-HT2AR activation to cortical neuron growth have not been fully elucidated, they are likely to involve AMPA receptor, TrkB, and mTOR signaling, as previously established (9). Future studies should examine the detailed signaling interplay between these proteins.

In addition to promoting psychedelic-induced structural neuroplasticity, the intracellular population of 5-HT2ARs might also contribute to the hallucinogenic effects of psychedelics. When we administered a serotonin-releasing agent to WT mice, we did not observe a HTR. However, the same drug was able to induce a HTR in mice that expressed SERT on cortical

neurons of the mPFC, a brain region that is known to be essential for the HTR (49). Thus, activation of intracellular cortical 5-HT2ARs may play a role in the subjective effects of psychedelics. This hypothesis is further supported by previous work that demonstrates that a high dose of the serotonin precursor 5-hydroxytryptophan (5-HTP) induces a HTR in WT mice, which can be blocked by an N-methyltransferase inhibitor that prevents the metabolism of 5-HTP to N-methyltryptamines (50). Inhibition of N-methyltransferase failed to block the HTR induced by 5-MeO–DMT (50). Taken together, this work emphasizes that accessing intracellular 5-HT2ARs is important for 5-HT2AR agonists to produce a HTR.

Our results demonstrate that membrane permeability is essential for a ligand to activate 5-HT2ARs in cortical neurons; however, our experiments did not distinguish between intracellular signaling or the possibility of psychedelics acting as pharmacological chaperones. Others have hypothesized that GPCR ligands may act as pharmacological chaperones, which facilitates their export to the plasma membrane where they could presumably engage in canonical signaling (51). Thus, future studies should

determine whether intracellular 5-HT2AR signaling is distinct from 5-HT2AR signaling at the plasma membrane.

Although intracellular expression of 5-HT2ARs within cortical pyramidal neurons has been known for some time, it is unclear at present why the subcellular localization of these receptors differs greatly between neurons and HEK293T cells (28, 29, 31). One possibility is that 5-HT2ARs form heterodimeric complexes that affect cellular trafficking (31). Thus, by dictating 5-HT2AR localization, cellular context could influence responses to endogenous neuromodulators and/or exogenous drugs, which potentially results in circuit-specific effects of 5-HT2AR ligands.

Intracellular signaling has been hypothesized to contribute to the pharmacological properties of a diverse range of compounds that includes nicotine, ketamine, and SSRIs (51–53). Like psychedelics, these compounds are weak bases with pK_a (where K_a is the acid dissociation constant) values ranging from 7 to 10. Given that the antidepressant mechanisms of ketamine and SSRIs have not been definitively established, it is intriguing to speculate that they also might promote cortical neuron growth

Fig. 5. Cellular uptake of serotonin produces antidepressant-like effects in vivo. (**A**) Schematic that displays experimental design for measuring spine density in Thy1-EGFP mice after administration of a serotonin-releasing agent. (**B**) Histology images of the mPFC of Thy1-EGFP mice that express CaMKII-mCherry or CaMKII-SERT-mCherry. (**C**) Confocal images of dendritic spines in the mPFC of mice treated with PCA (5 mg/kg ip). (**D**) Mice that express CaMKII-SERT-mCherry display increased dendritic spine density after PCA treatment. (**E**) Schematic that displays experimental design for determining the sustained antidepressant-like effects of serotonin in mice that express SERT in the mPFC. (**F**) NIL demonstrates no difference between CaMKII-SERT-EYFP– and CaMKII-GFP–expressing mice. (**G**) CaMKII-SERT-EYFP– and CaMKII-GFP–expressing mice exhibit no differences in the FST. After PCA (5 mg/kg ip) administration, CaMKII-SERT-EYFP–expressing mice display a sustained antidepressant-like effect. ns is not significant, $*p < 0.05$, and $**p < 0.01$, as compared between indicated pairs of data in (D) and (F) (two-tailed unpaired Student's t test) or (G) (two-way repeated measures ANOVA followed by Šídák's multiple comparisons test). Error bars in (D), (F), and (G) represent standard error of the mean.

by binding to intracellular targets. Perhaps other antidepressants affect the function of scaffolding proteins within the cell interior to modulate neuronal growth phenotypes.

Without facilitated transport across the plasma membrane, serotonin cannot induce psychedelic-like effects on neuronal morphology. Although it is possible that serotonin could alter cortical neuron physiology by activating cell-surface 5-HT2ARs, this receptor pool does not seem to be involved in 5-HT2AR–induced structural plasticity. Our results raise the intriguing possibility that serotonin may not be the endogenous ligand for the population of 5-HT2ARs expressed inside cortical neurons. Alternative ligands could include methylated congeners of serotonin or TRY because these compounds have greater abilities to cross nonpolar membranes. Endogenous psychedelics such as DMT, 5-MeO–DMT, and bufotenin have been identified in a variety of species, including humans, and have long been hypothesized to play roles in diseases such as schizophrenia (*54*). However, they are rapidly degraded in vivo, which makes their detection by classic analytical methods quite challenging. The use of more modern analytical techniques has improved detection of these analytes (*55*), with a recent study demonstrating that the concentration of DMT in the cortex was comparable to that of serotonin (*56*). The possibility that endogenous psychedelics play a role in health or disease should therefore be thoroughly investigated.

REFERENCES AND NOTES

1. R. S. Duman, G. K. Aghajanian, G. Sanacora, J. H. Krystal, *Nat. Med.* **22**, 238–249 (2016).
2. H. Qiao *et al.*, *Neural Plast.* **2016**, 8056370 (2016).
3. R. M. Shansky, C. Hamo, P. R. Hof, B. S. McEwen, J. H. Morrison, *Cereb. Cortex* **19**, 2479–2484 (2009).
4. T. Rantamäki *et al.*, *Neuropsychopharmacology* **32**, 2152–2162 (2007).
5. P. C. Casarotto *et al.*, *Cell* **184**, 1299–1313.e19 (2021).
6. D. E. Olson, *J. Exp. Neurosci.* **12**, 1179069518800508 (2018).
7. M. V. Vargas, R. Meyer, A. A. Avanes, M. Rus, D. E. Olson, *Front. Psychiatry* **12**, 727117 (2021).
8. A. C. Kwan, D. E. Olson, K. H. Preller, B. L. Roth, *Nat. Neurosci.* **25**, 1407–1419 (2022).
9. C. Ly *et al.*, *Cell Rep.* **23**, 3170–3182 (2018).
10. M. de la Fuente Revenga *et al.*, *Cell Rep.* **37**, 109836 (2021).
11. D. E. Olson, *Biochemistry* **61**, 127–136 (2021).
12. L. E. Dunlap *et al.*, *J. Med. Chem.* **63**, 1142–1155 (2020).
13. L. P. Cameron *et al.*, *Nature* **589**, 474–479 (2021).
14. C. Dong *et al.*, *Cell* **184**, 2779–2792.e18 (2021).
15. D. Cao *et al.*, *Science* **375**, 403–411 (2022).
16. L. M. Luttrell, S. Maudsley, L. M. Bohn, *Mol. Pharmacol.* **88**, 579–588 (2015).
17. K. Kim *et al.*, *Cell* **182**, 1574–1588.e19 (2020).
18. R. Irannejad *et al.*, *Nat. Chem. Biol.* **13**, 799–806 (2017).
19. M. A. Mohammad Nexhady, J. C. Nezhady, S. Chemtob, *iScience* **23**, 101643 (2020).
20. N. V. Weisstaub *et al.*, *Science* **313**, 536–540 (2006).
21. D. Ristanović, N. T. Milosević, V. Stulić, *J. Neurosci. Methods* **158**, 212–218 (2006).
22. B. J. Ebersole, I. Visiers, H. Weinstein, S. C. Sealfon, *Mol. Pharmacol.* **63**, 36–43 (2003).
23. R. H. J. Olsen *et al.*, *Nat. Chem. Biol.* **16**, 841–849 (2020).
24. J. C. Bermak, M. Li, C. Bullock, Q. Y. Zhou, *Nat. Cell Biol.* **3**, 492–498 (2001).
25. U. E. Petäjä-Repo, M. Hogue, A. Laperriere, P. Walker, M. Bouvier, *J. Biol. Chem.* **275**, 13727–13736 (2000).
26. S. E. Jacobsen *et al.*, *J. Biol. Chem.* **292**, 6910–6926 (2017).
27. C. A. Purgert *et al.*, *J. Neurosci.* **34**, 4589–4598 (2014).
28. V. Cornea-Hébert, M. Riad, C. Wu, S. K. Singh, L. Descarries, *J. Comp. Neurol.* **409**, 187–209 (1999).
29. V. Cornea-Hébert *et al.*, *Neuroscience* **113**, 23–35 (2002).
30. C. L. Schmid, K. M. Raehal, L. M. Bohn, *Proc. Natl. Acad. Sci. U.S.A.* **105**, 1079–1084 (2008).
31. R. Toneatti *et al.*, *Sci. Signal.* **13**, eaaw3122 (2020).
32. J. E. Saffitz, S. B. Liggett, *Circ. Res.* **70**, 1320–1325 (1992).
33. Q. Fu, Y. K. Xiang, *Prog. Mol. Biol. Transl. Sci.* **132**, 151–188 (2015).
34. A. C. Magalhaes *et al.*, *Nat. Neurosci.* **13**, 622–629 (2010).
35. J. L. Seachrist, S. S. Ferguson, *Life Sci.* **74**, 225–235 (2003).
36. C. A. Nash, W. Wei, R. Irannejad, A. V. Smrcka, *eLife* **8**, e48167 (2019).
37. R. Irannejad *et al.*, *Nature* **495**, 534–538 (2013).
38. M. Stoeber *et al.*, *Neuron* **98**, 963–976.e5 (2018).
39. S. Aggarwal, O. V. Mortensen, *Curr. Protocols Pharmacol.* **79**, 12.16.1–12.16.17 (2017).
40. F. C. Zhou, Y. Sari, J. K. Zhang, *Brain Res. Dev. Brain Res.* **119**, 33–45 (2000).
41. C. Lebrand *et al.*, *J. Comp. Neurol.* **401**, 506–524 (1998).
42. M. Fuchikami *et al.*, *Proc. Natl. Acad. Sci. U.S.A.* **112**, 8106–8111 (2015).
43. T. Sharp, T. Zetterström, L. Christmanson, U. Ungerstedt, *Neurosci. Lett.* **72**, 320–324 (1986).
44. R. N. Moda-Sava *et al.*, *Science* **364**, eaat8078 (2019).
45. D. A. Slattery, J. F. Cryan, *Nat. Protoc.* **7**, 1009–1014 (2012).
46. S. E. Crilly, W. Ko, Z. Y. Weinberg, M. A. Puthenveedu, *eLife* **10**, e67478 (2021).
47. C. Ly *et al.*, *ACS Pharmacol. Transl. Sci.* **4**, 452–460 (2020).
48. L. X. Shao *et al.*, *Neuron* **109**, 2535–2544.e4 (2021).
49. J. González-Maeso *et al.*, *Neuron* **53**, 439–452 (2007).
50. C. L. Schmid, L. M. Bohn, *J. Neurosci.* **30**, 13513–13524 (2010).
51. H. A. Lester, J. M. Miwa, R. Srinivasan, *Biol. Psychiatry* **72**, 907–915 (2012).
52. B. J. Henderson, H. A. Lester, *Neuropharmacology* **96**, 178–193 (2015).
53. H. A. Lester, L. D. Lavis, D. A. Dougherty, *Am. J. Psychiatry* **172**, 1064–1066 (2015).
54. S. A. Barker, E. H. McIlhenny, R. Strassman, *Drug Test. Anal.* **4**, 617–635 (2012).
55. S. A. Barker, J. Borjigin, I. Lomnicka, R. Strassman, *Biomed. Chromatogr.* **27**, 1690–1700 (2013).
56. J. G. Dean *et al.*, *Sci. Rep.* **9**, 9333 (2019).
57. M. V. Vargas *et al.*, Data set for Intracellular 5-HT2A Paper, Figshare (2022); https://doi.org/10.6084/m9.figshare.21669635.

SUPPLEMENTARY MATERIALS

science.org/doi/10.1126/science.adf0435
Materials and Methods
Figs. S1 to S10
References (*58, 59*)
MDAR Reproducibility Checklist

View/request a protocol for this paper from *Bio-protocol*.

Psychedelics promote neuroplasticity through the activation of intracellular 5-HT2A receptors

Maxemiliano V. Vargas, Lee E. Dunlap, Chunyang Dong, Samuel J. Carter, Robert J. Tombari, Shekib A. Jami, Lindsay P. Cameron, Seona D. Patel, Joseph J. Hennessey, Hannah N. Saeger, John D. McCorvy, John A. Gray, Lin Tian, and David E. Olson

The mechanism underlying psychedelic action

Psychedelic compounds promote cortical structural and functional neuroplasticity through the activation of serotonin 2A receptors. However, the mechanisms by which receptor activation leads to changes in neuronal growth are still poorly defined. Vargas *et al.* found that activation of intracellular serotonin 2A receptors is responsible for the plasticity-promoting and antidepressant-like properties of psychedelic compounds, but serotonin may not be the natural ligand for those intracellular receptors (see the Perspective by Hess and Gould). —PRS

View the article online
https://www.science.org/doi/10.1126/science.adf0435
Permissions
https://www.science.org/help/reprints-and-permissions

Use of this article is subject to the Terms of service